

CFD Simulation of Mass Transfer Phenomena in Spacer Filled Channels for Reverse Electrodialysis Applications

Luigi Gurreri^a, Alessandro Tamburini^{*a}, Andrea Cipollina^a, Giorgio Micale^a, Michele Ciofalo^b

^aDipartimento di Ingegneria Chimica, Gestionale, Informatica, Meccanica - Università degli Studi di Palermo, Viale delle Scienze Edificio 6 - 90128 Palermo, Italy

^bDipartimento dell' Energia, Ingegneria, dell'Informazione e Modelli Matematici - Università di Palermo, Viale delle Scienze Edificio 6, 90128 Palermo, Italy
 alessandro.tamburini@unipa.it

Salinity Gradient Power via Reverse Electrodialysis is a topic of primary importance nowadays. It allows getting energy from the “controlled” mixing of solutions at different salt concentration. The performance of this technology depends on many factors such as: components properties (i.e. membranes, spacers, electrodes), stack geometry, operating conditions and feeds features. Concentration polarization phenomena may significantly affect the actual membrane potential, thus reducing the gross power produced. On the other hand, C-polarization phenomena may significantly be reduced by suitably choosing the hydrodynamic regime within the stack. Such a choice may in turn significantly require higher pumping power, thus reducing the net power output. In this work, carried out within the EU-FP7 funded REAPower project, CFD simulations were carried out in order to study the fluid flow behaviour and mass transport phenomena within spacer-filled channels for SGP-RE technology. The effect of different parameters (channel geometry, feed flow rate, feed solution concentration and current density) on concentration polarization was assessed. The well known unit cell approach was adopted for the simulations in order to reduce their computational requirements as well as to increase the level of detail. Results show that the electrical potential loss due to polarization phenomena should be regarded as little significant in the case of seawater-brine for the operating conditions and geometrical configurations investigated. Conversely, a great attention should be devoted to such phenomena when very diluted solutions are to be employed (e.g. river water).

1. Introduction

In recent years many efforts have been devoted to adopting renewable energy sources to drive conventional separation processes (Cipollina et al., 2011; Cipollina et al., 2012) or to simply produce electric current. In this regard, Salinity Gradient Power by Reverse Electrodialysis (SGP-RE) is a technology to draw electric energy from the mixing of solutions at different salt concentrations (Tedesco et al., 2012). In particular, SGP-RE allows the production of electricity from the different chemical potentials of two differently concentrated salty solutions flowing in alternate channels suitably separated by selective ion exchange membranes. In such processes, the ion exchange membranes adopted cause a difference between the ions mobility in the membrane phase and in the solution phase to arise thus resulting in concentration (C) gradients in the solution between the membrane surface and the well mixed bulk (diffusion boundary layer) (Strathmann, 2004). When C-polarization phenomena occur in reverse electrodialysis, an increased salt concentration at the membrane surface in the dilute channel and a decreased salt concentration at the membrane surface in the concentrate channel can be observed. The C-difference at the membrane-solution interfaces will be smaller than the concentration difference between the bulk solutions. As a consequence, the resulting electromotive force is lower than the Open Circuit Voltage (OCV) and a lower voltage over the stack is therefore obtained (Vermaas et al., 2012). Długołęcki et al. (2010) measured all the contributions to the resistance across an ionic exchange membrane (i.e.

pure membrane resistance, diffusion boundary layer and double layer). Experimental data revealed that at very low salt concentrations (0.017M NaCl), the dominant resistance is the diffusion boundary layer resistance, whereas the pure membrane resistance is of minor importance. At higher salt C (0.5M NaCl), the pure membrane resistance is the dominant resistance, but even at this C the diffusion boundary layer plays a considerable role.

Although some efforts have been done so far to experimentally measure or estimate the concentration polarization, the literature is still lacking a suitable model of transport phenomena in channels for reverse electro dialysis. In this regard, Brauns (2009) proposed a model, which takes also into account the concentration polarization, to evaluate the effect of various parameters on electrical power output. However, Brauns claimed that no suitable model is available to calculate the boundary layer thickness.

Moreover, all the experimental information available so far on transport phenomena in SGP-RE units are relevant to the adoption of seawater and river water as feed solutions while no specific study on this topic has been carried out for the mixing case of seawater and brine. This condition is investigated (within the REAPower project) as a possible effective alternative to the traditional one where the dilute channel resistance (the one including the river water) is dramatically high.

The purpose of this work is to assess concentration polarization via CFD modelling of transport phenomena in spacer-filled channels for reverse electro dialysis. The influence of parameters as flow rate, concentration (brine, seawater and river water), molar flux through membranes (i.e. current density) and spacer geometry will be evaluated by means of a suitable model.

2. Simulated systems

Different configurations of reverse electro dialysis channels were investigated via CFD simulations: i) empty (i.e. spacer-less) channel with thickness equal to 400 μm ; ii) spacer-filled channels: woven 400 μm (ideal spacer), DelStar Naltex and Deukum (commercial spacers), whose features are shown in Figure1. The linear flow velocities (and corresponding pressure drops) tested range from 0.1 to 14.31 cm/s. Different NaCl feed solutions at 25 $^{\circ}\text{C}$ were simulated: brine 5 M, seawater 0.5 M and river water 0.017M. The diffusivity of NaCl in aqueous solutions was derived from the data by Vitagliano and Lyons (1955). Table1 summarizes the physical properties of the NaCl solutions studied by the CFD simulations.

Table 1: Physical properties of NaCl aqueous solutions at 25 $^{\circ}\text{C}$.

	Molarity [mol/l]	Density [kg/l]	Viscosity [cP]	Diffusivity of NaCl [m^2/s]
Brine	5.0	1.1828	1.660	1.580e-09
Seawater	0.5	1.0172	0.9312	1.472e-09
River water	0.017	0.9977	0.8913	1.533e-09

3. Modelling and numerical details

All CFD simulations were carried out by using the commercial code *CFX13* (Ansys®). Continuity and momentum equations of a Newtonian and incompressible fluid were solved via the CFD code. Full details can be found in Gurreri et al. (2012). According to Newman (1991), the electrolyte transport equation can be obtained from the rigorous Stefan-Maxwell equation along with the assumptions of (i) binary electrolyte and (ii) local electroneutrality condition:

$$\frac{\partial C}{\partial t} + \vec{\nabla} \cdot (C \vec{u}_0) = \vec{\nabla} \cdot \left[D \left(1 - \frac{d \ln C_0}{d \ln C} \right) \vec{\nabla} C \right] - \frac{\vec{i} \cdot \vec{\nabla} t_i^0}{z_i \nu_i F} \quad (1)$$

where C is the electrolyte concentration, u_0 is the solvent velocity, D is the salt diffusivity, C_0 is the solvent concentration, \vec{i} is the current density, t_i^0 is the transference number with respect to the solvent velocity, z_i is the valence, ν_i is the number of moles of dissociation (=1 in our cases) and subscript i refers to either cation or anion.

The contribution of the migrative term $\vec{i} \cdot \vec{\nabla} t_i^0 / z_i \nu_i F$ was separately assessed: the electrolyte concentration distribution was preliminarily obtained by employing the diffusive and convective terms contribution only. On this basis, the migrative term in Eq (1) was calculated a posteriori: it resulted to be at least five orders of magnitude lower than the diffusive and convective contributions, suggesting that this term can be reasonably neglected. Also, the practical aim of the present work is reliably estimating the concentration polarization phenomena rather than accurately predicting all the features, including also the most

negligible, of the ions transport within SGP-RE stacks. Notably, the transport number is dependent on concentration distribution and it was calculated in accordance with the relation by Smits and Duyvis (1965).

By assuming a linear variation of density with concentration (i.e. $\rho = aC + b$) the diffusivity correction term was substituted by a simpler expression

$$\frac{\partial C}{\partial t} + \vec{\nabla} \cdot (C\vec{u}_0) = \vec{\nabla} \cdot \left[D \frac{b}{b + (a - M)C} \vec{\nabla} C \right] \quad (2)$$

where M is the salt molecular weight.

As usually done in the literature, only one channel was simulated in each CFD simulation (either the concentrated or the dilute channel) by employing the unit cell approach along with typical boundary conditions (Tamburini et al., 2012). Clearly, the computational domain where the concentration and the velocity fields are to be simulated does not include the membrane. Figure 1 shows the Unit Cells adopted for the various channel-configurations.

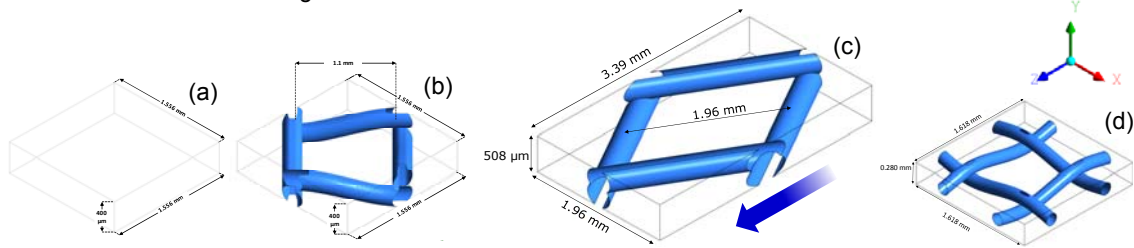


Figure 1: Unit cell for the (a) empty channel, (b) woven, (c) DelStar Naltex and (d) Deukum spacer-filled channels.

As a matter of fact, the CFD software does not implement the fully-developed mass transfer boundary condition: it does not allow setting boundary conditions by imposing a concentration gradient between the periodic surfaces of the unit cell. Therefore, some modifications were needed for the Eq (2).

A periodic unit-cell is, by definition, characterized by a fully developed fluid flow where concentration can be assumed to vary linearly along the main flow direction. By defining \hat{C} as the periodic concentration and z as the main flow direction coordinate:

$$C = \hat{C}(x, y, z, t) - kz = \dots = \hat{C}(x, y, z, t) - \frac{Q_{tot}}{V\bar{w}} z \quad (3)$$

The value of k can be devised from the mass balance, V is volume, \bar{w} is average value of the velocity z -component (at the z -section), Q_{tot} is the total molar flow rate through the membranes. The periodic concentration \hat{C} is the variable which has to be transported in the unit cell approach. Clearly, \hat{C} takes the same values in the *inlet* and *outlet* section of the unit cell and the transport equation must be modified accordingly by substituting Eq(3) in Eq(2):

$$\frac{\partial \hat{C}}{\partial t} + \vec{\nabla} \cdot (\hat{C}\vec{u}_0) = \vec{\nabla} \cdot \left[D \frac{b}{b + (a - M)(\hat{C} - kz)} \vec{\nabla} \hat{C} \right] + kw \quad (4)$$

Eq(3) was then adopted to get the real concentration field within the channel. Practically, the source term kw is devoted to restore the mass balance in the computational domain. As a matter of fact, adopting periodic conditions for the scalar and setting coming out fluxes across the membranes would produce a mass imbalance thus leading the CFD simulations to diverge. Notably, when the dilute channel has to be simulated, the ions flux is entering the domain and the signs of the terms containing k of Eq (3) and Eq (4) must be changed. This whole procedure is often employed in the literature for the scalar temperature transport (Di Liberto and Ciofalo, 2013). The results obtained by adopting the unit cell approach were validated (not show for brevity) by employing a wider computational volume composed of a number of unit cells.

As far as the discretization of the computational volume is concerned, a *grid size sensitivity analysis* was performed and a maximum discrepancy in fluid flow field of only 3% between the adopted grids (~1 million

of computational volumes) and the finest ones tested (~2 millions) was obtained. Either completely hexahedral or hybrid grids were employed as suggested by Tamburini et al. (2012).

Translational periodic boundary conditions were imposed on the surfaces perpendicular to the fluid flow direction (Z-axis) and on the surfaces perpendicular to the X-axis. A pressure gradient (ΔP) is imposed on the formers thus allowing the fluid to move along the z-direction (Tamburini et al., 2012). Spacer filament surfaces were considered as walls along with no-slip boundary conditions and no flux. The surfaces perpendicular to the Y-axis represent the membrane-solution interfaces and they were defined as walls with no-slip boundary conditions. Also, either coming out or entering fluxes for the electrolyte were imposed on these membrane surfaces of either the concentrated or the dilute channel, respectively. A homogeneous flux was imposed, corresponding to a current density ranging from 30 to 200 A/m². The lowest values of current density were equal to those obtained in a laboratory stack 10x10 cm² composed by 50 cell pairs (Veerman et al., 2009). Conversely, the highest values should be considered as provisional (or very conservative) values achievable in systems optimized for high power density outputs. Concentration polarization phenomena are usually quantified via suitable *polarization factors* θ defined as the ratio between the bulk and membrane-solution interface concentration. In formula:

$$\theta = \frac{C_i}{C_b} \text{ for the concentrated channel ; } \theta = \frac{C_b}{C_i} \text{ for the dilute channel} \quad (5)$$

where C_i is the mean concentration in the membrane-solution interfaces, and C_b is the mean concentration in the *bulk plane* (a plane parallel to the membrane-solution interfaces, placed midway between the two membranes). In relation to the definitions of Eq(5), θ is always lower than 1, and the higher the θ value, the less significant the polarization phenomenon.

The High Resolution Scheme was used for the discretization of the convective terms and shape functions were used to evaluate spatial derivatives for all the diffusion terms. A coupled algorithm was adopted for the pressure-velocity coupling. Laminar steady state simulations were performed as the regime was found to be laminar at all the flow rates investigated. The number of iterations was chosen in order to guarantee that all the round mean square residuals settle at values lower than 10⁻⁶.

4. Results and discussion

4.1 Influence of concentration, velocity and current density on polarization phenomena

For the sake of brevity, in this section only the results relevant to the mostly adopted Deukum spacer filled channel will be provided. A comparison of the polarization-performances of other spacers (i.e. effect of spacer geometry on polarization) will be presented in section 4.2. Figure 2 shows the polarization factor trends as a function of the mean velocity along the main flow direction at different current densities for the case of channels fed by brine, seawater or river water. It is worth noting that the polarization factor is always very close to one ($\theta > 0.9$) when either brine or seawater are simulated. Conversely, it reaches significantly lower values ($\theta \approx 0.4-0.84$) for the case of the river water.

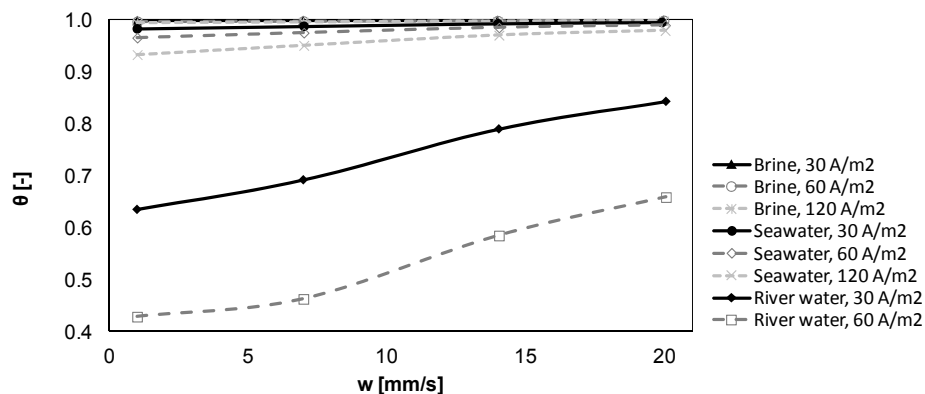


Figure 2: θ vs fluid velocity for Deukum spacer-filled channel for different feed solutions and i .

Therefore, at a given flow rate and current density, the higher the mean concentration of the feed solution, the higher the polarization factor. This is not surprising since the imposed flux and the corresponding ion

mass crossing the membranes is the same, but it corresponds to a lower percentage when the bulk concentration is higher. Also, the higher the current density (i.e. the higher the flux imposed at the membranes), the lower the value of θ although such a dependence is crucial only in the case of the river water. Eventually, the figure shows that a higher flow rate of the feed solution corresponds to an enhanced mixing within the channel leading polarization phenomena to decrease. Therefore, our findings confirm that polarization phenomena can be reduced by carefully optimizing fluid dynamics within the stack.

4.2 Comparison among spacer-filled and spacer-less channels

A representative example of the results collected is provided in Figure 3: it shows the concentration contours for different channels fed by seawater (as dilute solution) at a given pressure drop and current density. Clearly, in this case, the ion flux is entering the channel and the concentration is higher in the membrane-solution interfaces than in the bulk. In all cases of Figure 3 it can be observed that the concentration polarization is far from being significant. However, the presence of the net spacer appears to have a clear influence on concentration distribution by enhancing convective transport and reducing polarization consequently. Notably, also in this case a very high value of current density was adopted for the CFD simulations aiming at assessing the polarization in conservative/provisional conditions.

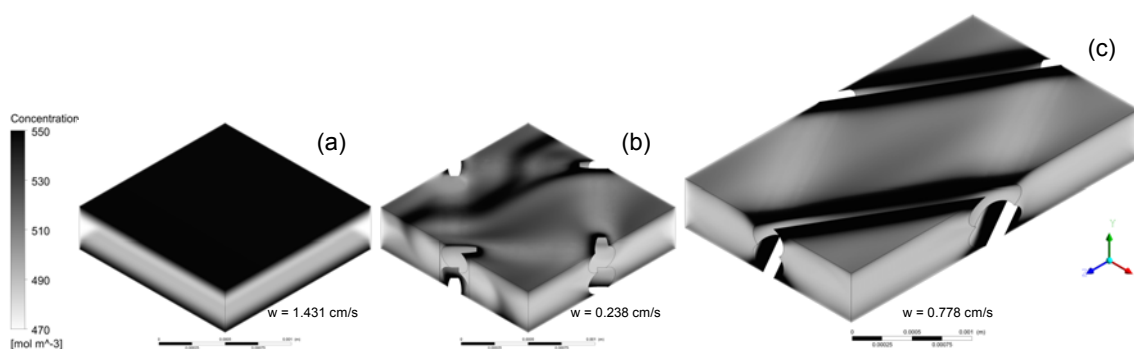


Figure 3: Concentration distribution for (a) empty channel ($400\ \mu\text{m}$ thick), (b) woven and (c) DelStar Naltex spacer-filled channels fed by seawater at the imposed pressure drop of $0.01\ \text{bar/m}$ and $i = 200\ \text{A/m}^2$.

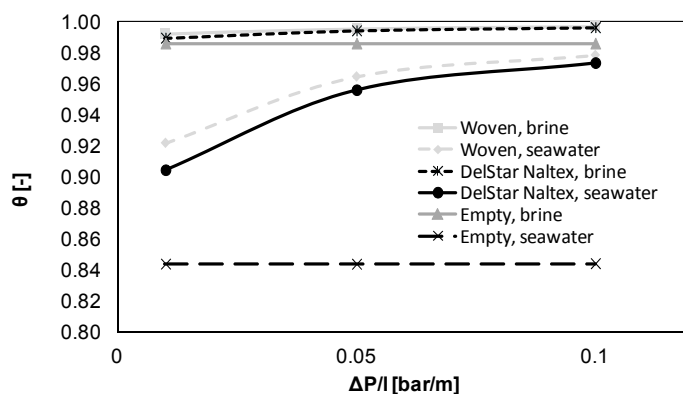


Figure 4: Polarization factor as a function of pressure drop for empty channel, woven and DelStar Naltex spacer-filled channels fed by either seawater or brine at a current density of $200\ \text{A/m}^2$.

Figure 4 reports the trend of the polarization factor θ as a function of the imposed pressure drops (along the main flow direction, z) for the case of brine-seawater fed in the empty channel, woven and DelStar Naltex spacer-filled channels again at a current density equal to $200\ \text{A/m}^2$. Also the results of Figure 4 suggest that polarization is not a crucial phenomenon at REAPower conditions (brine-seawater), especially in the brine channel even at very high current densities. It is worth noting that the increase of pressure drops does not yield a θ enhancement in the empty channel. This is due to the fact that the flow regime is perfectly laminar so that mixing due to turbulence does not occur and only the z -component of velocity is present (velocity component perpendicular to membranes is nil at all pressure drops tested). Conversely, a performance enhancement as the pressure drops increase can be observed when a spacer is included

within the channel as expected. Such velocities increase as the flow rate increases. Moreover, a similar polarization factor enhancement with imposed pressure drops was found for the two spacers investigated.

5. Conclusions

For the first time, CFD simulations were carried out to study concentration polarization phenomena in reverse electrodialysis channels. A transport equation suitable for concentrated solutions was purposely implemented in the commercial CFD code Ansys® CFX 13. Polarization phenomena were found to greatly decrease as the solution concentration increases. In particular, concentration polarization was found to be poorly significant for the case of seawater and practically negligible for the brine. Conversely, it should be taken into full account for the case of the river water where a very low polarization factor (i.e. high polarization) was predicted.

For all the cases investigated, the higher the current density, the lower the polarization factor. However, operating the SGP-RE stack at REAPower conditions (i.e. brine – seawater) even very high current densities do not yield large polarizations, especially for the brine channel case. Conversely, it would lead to a deep polarization if the river water was employed as diluted solution.

Notwithstanding the fluid flow regime was laminar for all the CFD simulations, the flow rate was found to influence polarization phenomena. This is due to the lack of auto-similarity (Tamburini et al., 2012) of the flow field and to the presence of velocity components perpendicular to the membranes: all the factors promoting fluid mixing within the channel (i.e. the presence of a net spacer and/or the increase of feed flow rate) were found to enhance the polarization factor, even if, on the other hand, they also lead to increased pressure drops. No effect of flow rate on θ was observed for the empty channel where the flow is auto-similar and no velocity component perpendicular to the membrane is present. However, the influence of the spacer type does not appear to be crucial at REAPower conditions.

Summarizing, polarization phenomena should be regarded as little significant in the case of seawater-brine for practically all the operating conditions and geometrical configurations investigated in the present paper.

References

- Brauns E., 2009, Salinity gradient power by reverse electrodialysis: effect of model parameters on electrical power output, *Desalination*, 237, 378–391.
- Cipollina A., Di Sparti M.G., Tamburini A., Micale G., 2012, Development of a Membrane Distillation module for solar energy seawater desalination, *Chem. Eng. Res. & Des.*, 90, 2101-2121.
- Cipollina A., Micale G., Noto S., Brucato A., 2011, Multi stage flash desalination with direct mixing condensation, *Chemical Engineering Transactions*, 24, 1555-1560.
- Di Liberto M., Ciofalo M., 2013, A study of turbulent heat transfer in curved pipes by numerical simulation, *International Journal of Heat and Mass Transfer*, 59, 112–125.
- Długołęcki P., Ogonowski P., Metz S.J., Saakes M., Nijmeijer K., Wessling M., 2010, On the resistances of membrane, diffusion boundary layer and double layer in ion exchange membrane transport, *Journal of Membrane Science*, 349, 369–379.
- Gurreri L., Tamburini A., Cipollina A., Micale G., 2012, CFD analysis of the fluid flow behaviour in a reverse electrodialysis stack, *Desalination and Water Treatment*, 48, 390-403.
- Newman J.S., 1991, *Electrochemical Systems*, 2nd edition, Prentice Hall, Englewood Cliffs, NJ: , USA, Prentice Hall.
- Smits L.J.M., Duyvis E.M., 1966, Transport numbers of concentrated sodium chloride solutions at 25°, *The Journal of Physical Chemistry*, 70, 2747–2753.
- Strathmann, H., 2004, Ion-exchange membrane separation processes, *Membrane Science and Technology Series*, 9.
- Tamburini A., La Barbera G., Cipollina A., Ciofalo M., Micale G., 2012, CFD simulation of channels for direct and reverse electrodialysis, *Desalination and Water Treatment*, 48, 370–389.
- Tedesco M., Cipollina A., Tamburini A., van Baak W., Micale G., 2012, Modelling the Reverse ElectroDialysis process with seawater and concentrated brines, *Desalination and Water Treatment*, 49, 404–424.
- Veerman J., Saakes M., Metz S.J., Harmsen G.J., 2009, Reverse electrodialysis: Performance of a stack with 50 cells on the mixing of sea and river water, *Journal of Membrane Science*, 327, 136–144.
- Vermaas, D. A., Gulera, E., Saakes, M., Nijmeijer, K., 2012, Theoretical power density from salinity gradients using reverse electrodialysis, *Energy Procedia* 20, 170–184.
- Vitagliano V., Lyons P.A., 1956, Diffusion Coefficients for Aqueous Solutions of Sodium Chloride and Barium Chloride, *Journal of American Chemical Society*, 78, 1549-1552.